1 kHz nanosecond-pulsed room temperature Fe:ZnSe laser gain-switched by a ZnGeP₂ optical parametric oscillator

Yingyi Li (李英一), **Ke Yang** (杨 科), **Gaoyou Liu** (刘高佑), **Baoquan Yao** (姚宝权)*, **and Youlun Ju** (鞠有伦)

National Key Laboratory of Tunable Laser Technology, Harbin Institute of Technology, Harbin 150001, China
*Corresponding author: yaobq08@hit.edu.cn

We demonstrate a Fe:ZnSe laser gain-switched by a ZnGeP₂ optical parametric oscillator (OPO) under the pulse repetition frequency of 1 kHz at room temperature. The 2.9 μm signal light of the OPO is employed as the pump for the Fe:ZnSe laser. The maximum output power of the Fe:ZnSe laser is 58 mW with the pulse duration of 2.7 ns under the incident pump power of 280 mW, corresponding to a peak pulse power of 21.5 kW and an optical-to-optical efficiency of 20.7%. The spectrum of the Fe:ZnSe laser has a range of 4030.2–4593.6 nm with a dip at 4187.1–4340.4 nm due to the absorption of CO_2.

OCIS codes: 140.3070, 140.3295.
doi: 10.3788/COL201917.081404.

The 3–5 μm lasers are widely used in a lot of fields such as remote sensing, laser radar, spectrum analysis, environment monitoring, medical treatment, and military applications[1]. There are two major techniques to obtain lasers in this spectrum range. The optical parametric oscillator (OPO) is one promising technique. As the ZnGeP₂ (ZGP) crystal has the highest nonlinear coefficient (75 pm/V) and highest thermal conductivity (35 W/mK) among the 2-μm-pumped OPO materials[2], many researchers have made a lot of work on the 3–5 μm ZGP-OPOs[3–5]. Haakestad *et al.* reported a ZGP-based master oscillator power amplifier (MOPA) with the highest single pulse energy of 212 mJ in 2014[3], and Qian *et al.* reported a ZGP-based MOPA with the highest average power of 102 W in 2019[4].

The Fe:ZnSe laser is the other promising technique, and the Fe:ZnSe crystal has attracted a lot of attention because it has broad emission spectrum and high thermal conductivity, and could generate the lasing directly[9]. The first Fe:ZnSe laser was demonstrated at a liquid nitrogen temperature in 1999 by Adams *et al.*[10], and the laser has reached an output energy of 10.6 J, also under liquid nitrogen cooling pumped by free running Er-doped yttrium aluminum garnet (Er:YAG) radiation in 2016 that was achieved by Kozlovsky *et al.*[11]. Compared with the low temperature operation, the room temperature operation is more difficult to realize, because the lifetime of the upper laser state $^5T_2$ of Fe^{2+} drops from 68 μs at 77 K down to 382 ns at room temperature as a result of multiphonon quenching[12], which leads to a strong requirement of the sharp pumps. However, the appropriate sharp pumps around 3 μm, which are located near the absorption peak of the Fe:ZnSe crystal, are limited. In regard to low pulse repetition frequency (PRF) operation, the Fe:ZnSe lasers were mostly pumped by the hydrogen fluoride (HF)

lasers[13–22] and flash-lamp-pumped *Q*-switched Er:YAG, Er,Cr-doped yttrium scandium gallium garnet (Er,Cr: YSGG), and Er:YSGG lasers[23–30] with pulse durations of tens of nanoseconds. In regard to high PRF operation, Mirov *et al.* demonstrated a 1 kHz gain-switched Fe:ZnSe laser pumped by a 2.7 μm Cr:ZnSe radiation in 2015, where the output power, pulse duration, and spectrum width were 1 W, 5 ns, and 20 nm, respectively[9]. Besides, the high PRF Fe:ZnSe laser could be pumped by the ZGP-OPO. The ZGP-OPO pumped by Ho:YAG radiation can generate the signal light in the range of 2.6–3.1 μm, which is located in the absorption band of the Fe:ZnSe crystal. Using the ZGP-OPO as the pump for the Fe:ZnSe laser has another advantage that the corresponding idler light is in the range of 6.5–10.1 μm, which could be used in many specific applications such as laser jamming, laser guidance, obstacle avoidance, as well as in detecting chemical warfare and toxic industrial chemicals[31,32]. It means that we can obtain dual-wavelength radiation in the mid and far infrared regions.

In 2015, our team briefly reported a 1 kHz gain-switched Fe:ZnSe laser pumped by a ZGP-OPO within 400 Chinese characters[33]. The output power, pulse duration, and wavelength were 53 mW, 25 ns, and 4.33–4.61 μm, respectively. Nevertheless, the slope efficiency was only 4.8% due to an inappropriately long cavity, which caused a large diffraction loss. Meanwhile, the wavelength range was measured with a manual handwheel monochromator, and only eight wavelength points were collected, which led to a missing detail[33]. Limited by the paper length, the experimental process and results were not detailed, and there were no figures of the laser output characteristics either. So it is necessary to improve the experiment and write a full length paper to report the latest results.

In this Letter, we demonstrate a gain-switched Fe:ZnSe laser pumped by a 2.9 μm ZGP-OPO under the PRF of

1 kHz at room temperature. Under the incident pump power of 280 mW, a maximum output power of 58 mW is obtained with the pulse duration of 2.7 ns, corresponding to a peak pulse power of 21.5 kW and an optical-to-optical efficiency of 20.7%. The spectrum has a range of 4030.2–4593.6 nm, owning a dip in the range of 4187.1–4340.4 nm due to the absorption of CO_2.

The optical scheme of the ZGP-OPO and Fe:ZnSe laser is shown in Fig. 1. An electro-optical Q-switched Ho:YAG laser with the wavelength of 2.1 μm working under the PRF of 1 kHz was employed as the pump for the ZGP-OPO. The ZGP crystal was cut for Type II phase-matching with $\theta = 68.7°$, $\varphi = 90°$ relative to the optical axis, and the calculated signal light wavelength was 2.9 μm[34]. It was placed in a four-flat-mirror rectangle cavity. The output mirror of the idler light was coated with a transmittance of 25% at 6300–8300 nm, and the other three mirrors were coated with high transmissivity at 2000–2200 nm and 2600–3200 nm, and high reflectivity at 6300–8300 nm. Although this four-mirror structure increased the loss in the cavity and reduced the efficiency of the OPO, the Fresnel number was reduced, which led to a better beam quality. Meanwhile, the feedback to the pump source was eliminated.

The maximum signal light power of the ZGP-OPO was 280 mW, measured with an Ophir power meter (power range: 0.1 mW–10 W). The pulse duration at the maximum power was 18.2 ns, detected by a HgCdTe photodiode (wavelength range: 2000–10,600 nm, response time: 2 ns) and recorded with a LeCroy Wavesurfer 64Xs digital oscilloscope (bandwidth: 600 MHz, sampling rate: 2.5 GS/s), as shown in Fig. 2.

The wavelength of the signal light was 2.9 μm, measured with a home-made auto-scan monochromator (resolution: 0.3 nm), as shown in Fig. 3.

The Fe:ZnSe crystal was 10 mm × 10 mm in cross-section and 4 mm in thickness. It was grown by high-pressure vertical zone melting, and the Fe^{2+} doping concentration was 5×10^{18} cm^{-3}. The working cross-sections of the crystal were fine polished with a parallel degree within 30″. The crystal was wrapped by indium foil and mounted in a copper heat sink, the temperature of which was controlled with a thermoelectric cooler.

Figure 4 shows the absorptivity of the Fe:ZnSe crystal, measured with a PerkinElmer Spectrum ONE spectrometer in the range of 1500–5000 nm. The crystal had a broad
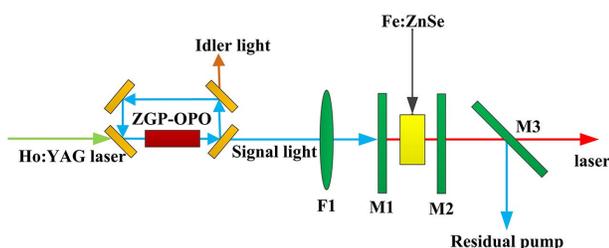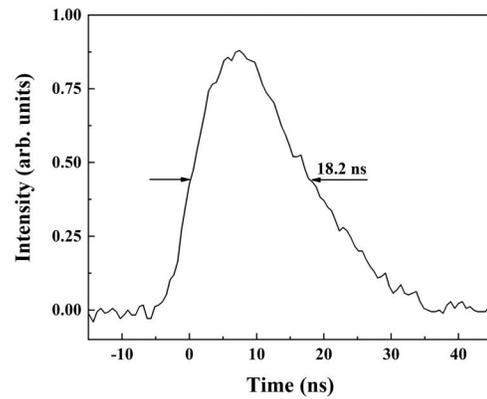
Fig. 2. Signal light temporal profile of the ZGP-OPO.
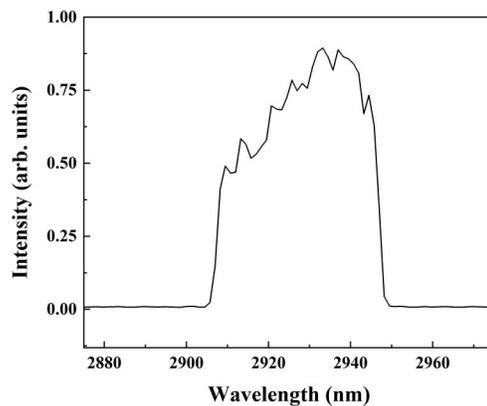
Fig. 3. Signal light spectrum of the ZGP-OPO.
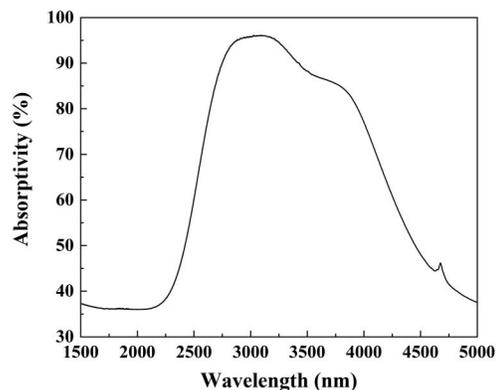
Fig. 4. Absorptivity of the Fe:ZnSe crystal.

absorption band, and the 2.9 μm signal light of the ZGP-OPO was just located near the peak of the curve.

The cavity of the Fe:ZnSe laser had a linear structure. The focus mirror F1, input mirror M1, output mirror M2, and dichroic mirror M3 were made of CaF_2. M1 was coated with high transmissivity at 2700–3100 nm and high reflectivity at 3800–4700 nm; M2 was coated with different transmittances at 3800–4700 nm; the 45° mirror M3 was coated with high transmissivity at 3800–4700 nm and high reflectivity at 2700–3100 nm, which was used

Fig. 1. Scheme of the ZGP-OPO and Fe:ZnSe laser.

to separate the residual pump. The 2.9 µm pump was focused by F1 and injected into the crystal along the optical axis of the installation.

Figure 5 shows the dependence of the output power on the incident pump power at the same transmittance, but different curvature radii of the output couplers and different cavity lengths at the PRF of 1 kHz at 18°C. T, R, L represent the transmittance, curvature radius of the output coupler, and the cavity length, respectively. The power was measured with the same power meter as that used in the ZGP-OPO.

When the cavity length was fixed to be 15 mm, the output power with the plano-concave output coupler of $T = 30\%$, $R = -100$ mm was higher than that of $T = 30\%$, $R = \infty$. When the cavity length with the output coupler of $T = 30\%$, $R = -100$ mm was changed, the output power with $L = 15$, 20, and 25 mm decreased in proper sequence. The maximum output power of 58 mW was acquired when the output coupler of $T = 30\%$, $R = -100$ mm was employed with $L = 15$ mm, corresponding to an optical-to-optical efficiency of 20.7%.

The pulse shape of the Fe:ZnSe laser was detected and recorded with the previous equipment. The pulse duration was 2.7 ns at the maximum output power of 58 mW, which was the shortest pulse duration of the Fe:ZnSe laser ever reported as far as we knew, corresponding to a peak pulse power of 21.5 kW, as shown in Fig. 6. Moreover, we recorded the laser and pump simultaneously, and a typical time delay between them is shown in Fig. 7.

Figure 8 shows the wavelength of the Fe:ZnSe laser measured with the previous monochromator. More than 1000 points were collected between 4000 and 5000 nm. At the maximum output power of 58 mW, the spectrum covered a range of 4030.2–4593.6 nm. Owing to the adequate points, a dip in the range of 4187.1–4340.4 nm caused by the absorption of CO_2 could be observed.

Fig. 6. Temporal profile of the Fe:ZnSe laser.

(a)

(b)
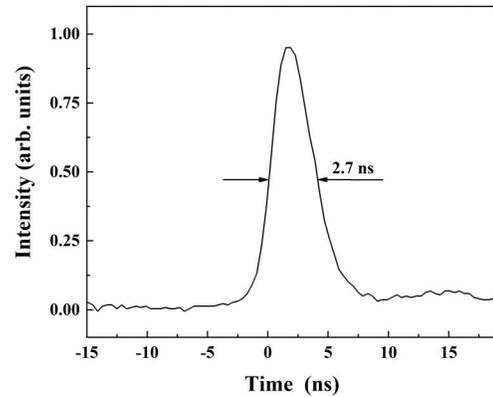
Fig. 5. Dependence of the output power on the incident pump power of the Fe:ZnSe laser.
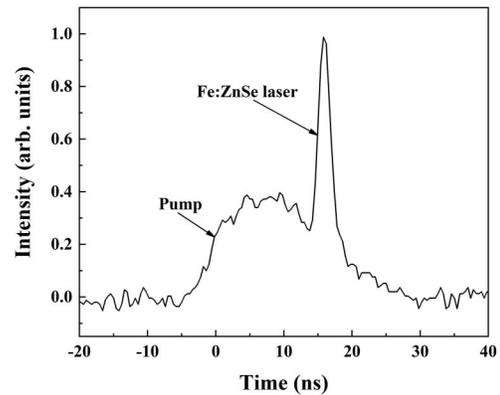
Fig. 7. Temporal profile of the Fe:ZnSe laser and pump.
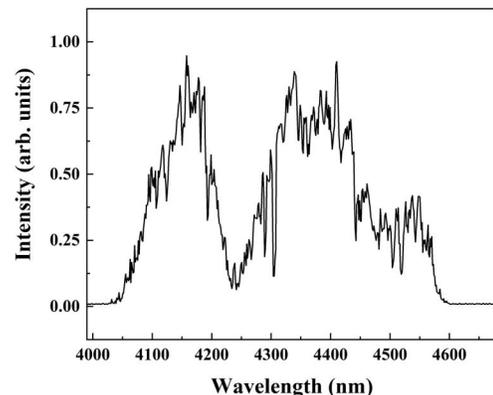
Fig. 8. Output spectrum of the Fe:ZnSe laser.
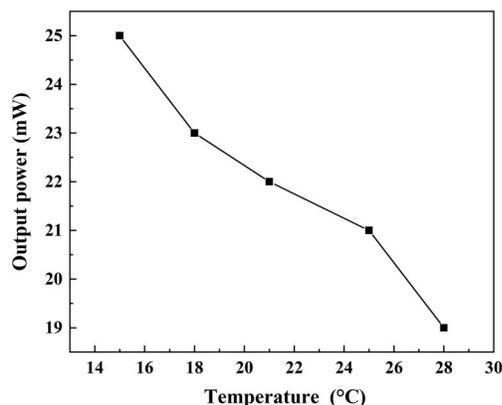
Fig. 9. Dependence of the output power on crystal temperature of the Fe:ZnSe laser.

Figure 9 shows the dependence of output power on the crystal temperature. They changed on the contrary among the five points between 15°C and 28°C, as the lifetime of $^5T_2$ decreases with the increasing temperature.

In conclusion, we have reported a room temperature Fe:ZnSe laser gain-switched by a ZGP-OPO. The maximum output power is 58 mW with pulse duration of 2.7 ns under the PRF of 1 kHz, corresponding to a peak pulse power of 21.5 kW and an optical-to-optical efficiency of 20.7%. The wavelength covers 4030.2–4593.6 nm with a dip in the range of 4187.1–4340.4 nm due to the absorption of CO_2.

Although the peak pulse power of 21.5 kW we obtained is not high compared with the ZGP-OPO[3,4], limited by the power of the 2.9 μm pump, we have demonstrated that this is a promising technique to obtain high PRF and short pulse duration 3–5 μm lasers. It is also the first, to the best of our knowledge, reported Fe:ZnSe laser with such high PRF and short pulse duration to date.

References

1. Z. P. Qin, G. Q. Xie, J. G. Ma, P. Yuan, and L. J. Qian, Chin. Opt. Lett. **15**, 111402 (2017).
2. P. G. Schunemann, K. T. Zawilski, L. A. Pomeranz, D. J. Creeden, and P. A. Budni, J. Opt. Soc. Am. B **33**, D36 (2016).
3. M. W. Haakestad, H. Fonnum, and E. Lippert, Opt. Express **22**, 8556 (2014).
4. C. P. Qian, B. Q. Yao, B. R. Zhao, G. Y. Liu, X. M. Duan, T. Y. Dai, Y. L. Ju, and Y. Z. Wang, Opt. Lett. **44**, 715 (2019).
5. E. C. Ji, M. M. Nie, and Q. Liu, Chin. Opt. Lett. **15**, 091402 (2017).
6. C. Kieleck, A. Berrou, B. Donelan, B. Cadier, T. Robin, and M. Eichhorn, Opt. Lett. **40**, 1101 (2015).
7. M. Schellhorn, G. Spindler, and M. Eichhorn, Opt. Lett. **42**, 1185 (2017).
8. M. Schellhorn, G. Spindler, and M. Eichhorn, Opt. Express **26**, 1402 (2018).
9. S. B. Mirov, V. V. Fedorov, D. Martyshkin, I. S. Moskalev, M. Mirov, and S. Vasilyev, IEEE J. Sel. Top. Quantum Electron. **21**, 292 (2015).
10. J. J. Adams, C. Bibeau, R. H. Page, D. M. Krol, L. H. Furu, and S. A. Payne, Opt. Lett. **24**, 1720 (1999).
11. V. I. Kozlovsky, Y. V. Korostelin, Y. P. Podmar'kov, Y. K. Skasyrsky, and M. P. Frolov, J. Phys. Conf. Ser. **740**, 012006 (2016).
12. N. Myoung, V. V. Fedorov, S. B. Mirov, and L. E. Wenger, J. Lumin. **132**, 600 (2012).
13. S. D. Velikanov, V. P. Danilov, N. G. Zakharov, N. N. Il'ichev, S. Y. Kazantsev, V. P. Kalinushkin, I. G. Kononov, A. S. Nasibov, M. I. Studenikin, P. P. Pashinin, K. N. Firsov, P. V. Shapkin, and V. V. Shchurov, Quantum Electron. **44**, 141 (2014).
14. E. M. Gavrishchuk, S. Y. Kazantsev, I. G. Kononov, S. A. Rodin, and K. N. Firsov, Quantum Electron. **44**, 505 (2014).
15. K. N. Firsov, E. M. Gavrishchuk, S. Y. Kazantsev, I. G. Kononov, and S. A. Rodin, Laser Phys. Lett. **11**, 085001 (2014).
16. K. N. Firsov, E. M. Gavrishchuk, S. Y. Kazantsev, I. G. Kononov, A. A. Maneshkin, G. M. Mishchenko, S. M. Nefedov, S. A. Rodin, S. D. Velikanov, I. M. Yutkin, N. A. Zaretsky, and E. A. Zotov, Laser Phys. Lett. **11**, 125004 (2014).
17. S. D. Velikanov, N. A. Zaretskiy, E. A. Zotov, V. I. Kozlovsky, Y. V. Korostelin, O. N. Krokhin, A. A. Maneshkin, Y. P. Podmar'kov, S. A. Savinova, Y. K. Skasyrsky, M. P. Frolov, R. S. Chuvatkin, and I. M. Yutkin, Quantum Electron. **45**, 1 (2015).
18. E. M. Gavrishchuk, V. B. Ikonnikov, S. Y. Kazantsev, I. G. Kononov, S. A. Rodin, D. V. Savin, N. A. Timofeeva, and K. N. Firsov, Quantum Electron. **45**, 823 (2015).
19. K. N. Firsov, M. P. Frolov, E. M. Gavrishchuk, S. Y. Kazantsev, I. G. Kononov, Y. V. Korostelin, A. A. Maneshkin, S. D. Velikanov, I. M. Yutkin, N. A. Zaretsky, and E. A. Zotov, Laser Phys. Lett. **13**, 015002 (2016).
20. K. N. Firsov, E. M. Gavrishchuk, V. B. Ikonnikov, S. Y. Kazantsev, I. G. Kononov, T. V. Kotereva, D. V. Savin, and N. A. Timofeeva, Laser Phys. Lett. **13**, 055002 (2016).
21. A. E. Dormidonov, K. N. Firsov, E. M. Gavrishchuk, V. B. Ikonnikov, S. Y. Kazantsev, I. G. Kononov, T. V. Kotereva, D. V. Savin, and N. A. Timofeeva, Appl. Phys. B **122**, 211 (2016).
22. S. D. Velikanov, N. A. Zaretsky, E. A. Zotov, S. Y. Kazantsev, I. G. Kononov, Y. V. Korostelin, A. A. Maneshkin, K. N. Firsov, M. P. Frolov, and I. M. Yutkin, Quantum Electron. **46**, 11 (2016).
23. V. A. Akimov, A. A. Vornonv, V. I. Kozlovsky, Y. V. Korosstelin, A. I. Landman, Y. P. Podmar'kov, and M. P. Frolov, Quantum Electron. **36**, 299 (2006).
24. M. E. Doroshenko, T. T. Basiev, P. Koranda, H. Jelínková, M. Němec, M. Čech, J. Šulc, V. K. Komar, A. S. Gerasimenko, V. V. Badikov, and D. V. Badikov, Proc. SPIE **7193**, 71931K (2009).
25. H. Jelínková, P. Koranda, M. E. Doroshenko, J. Šulc, M. Jelínek, M. Čech, T. T. Basiev, V. V. Badikov, and D. V. Badikov, Proc. SPIE **7721**, 772111 (2010).
26. M. E. Doroshenko, H. Jelinkova, P. Koranda, J. Sulc, T. T. Basiev, V. V. Osiko, V. K. Komar, A. S. Gerasimenko, V. M. Puzikov, V. V. Badikov, and D. V. Badikov, Laser Phys. Lett **7**, 38 (2010).
27. N. Myoung, D. V. Martyshkin, V. V. Fedorov, and S. B. Mirov, Opt. Lett. **36**, 94 (2011).
28. M. E. Doroshenko, H. Jelínková, T. T. Basiev, M. Jelínek, P. Koranda, M. Němec, V. K. Komar, A. K. Gerasimenko, V. V. Badikov, D. V. Badikov, D. Vyhlídal, and J. Stoklasa, Proc. SPIE **7912**, 79122D (2011).
29. H. Jelínková, M. E. Doroshenko, M. Jelínek, D. Vyhlídal, J. Šulc, M. Němec, V. Kubeček, Y. A. Zagoruiko, N. O. Kovalenko, A. S. Gerasimenko, V. M. Puzikov, and V. K. Komar, Proc. SPIE **8599**, 85990E (2013).

30. H. Jelínková, M. E. Doroshenko, M. Jelínek, J. Šulc, M. Němec, V. Kubeček, Y. A. Zagoruiko, N. O. Kovalenko, A. S. Gerasimenko, V. M. Puzikov, and V. K. Komar, Proc. SPIE **9342**, 93421V (2015).

31. M. E. Webber and M. Pushkarsky, J. Appl. Phys. **97**, 113101 (2005).

32. M. B. Pushkarsky, I. G. Dunayevskiy, M. Prasanna, A. G. Tsekoun, R. Go, and C. K. Patel, Proc. Natl. Acad. Sci. USA **103**, 19630 (2006).

33. B. Q. Yao, S. X. Xia, K. K. Yu, J. H. Yuan, and Y. J. Shen, Chin. J. Lasers **42**, 0119001 (2015).

34. Y. F. Peng, X. B. Wei, and W. M. Wang, Chin. Opt. Lett. **9**, 061403 (2011).